Polymer 51 (2010) 2779–2785

Contents lists available at ScienceDirect

Polymer

journal homepage: www.elsevier.com/locate/polymer

A DFT study on poly(lactic acid) polymorphs

Ting Ting Lin [a,b], Xiang Yang Liu [b], Chaobin He [a,*]

[a] Institute of Materials Research and Engineering, A*STAR (Agency for Science, Technology and Research), 3 Research Link, Singapore 117602
[b] Department of Physics, National University of Singapore, 2 Science Drive 3, Singapore 117542

ARTICLE INFO

Article history:
Received 28 January 2010
Received in revised form
30 March 2010
Accepted 31 March 2010
Available online 8 April 2010

Keywords:
DFT
Poly(lactic acid), polylactide
Non-conventional hydrogen bonding

ABSTRACT

Poly(lactic acid) (PLA) can crystallize in α-, β-, γ- and stereocomplex (sc)- forms. It has been shown that the formation of stereocomplex between poly(L-lactic acid) and poly(D-lactic acid) significantly improve thermal stability and mechanical properties. However the mechanisms of enhancements are still unclear. In this study, we investigate the PLA polymorphs from the first-principles theoretical perspective in order to understand the intermolecular interaction in the crystals. Density functional theory at the level of Perdew-Wang generalized-gradient approximation was applied to optimize PLA crystal unit cells. A comparison of energies in the various unit cells reveals that sc-form is the most energetically favorable form among the four PLA polymorphs. The order of thermodynamically relative stability is that sc-form is 0.3, 1.1, and 1.3 kcal/mol more stable than α-form, β-form, and γ-form, respectively (when using the ultrasoft pseudopotential and a plane-wave basis set with an energy cutoff of 380 eV) or 0.4, 1.1, and 1.3 kcal/mol more stable than α-form, β-form, and γ-form, respectively (when employing the density functional semi-core pseudopotentials and the double numerical plus polarization orbital basis set with a global orbital cutoff of 3.7 Å). In addition to the energetic properties, structural and electronic properties were calculated as well. The theoretical predicted stability rank is in agreement with some reported observations. Such as, sc-form has higher melting point and larger heat of fusion than those of α-form. The enhanced thermal stability of the sc-form compared to the other three homopolymer forms may be attributed to the unique intermolecular non-conventional hydrogen bonding C–H···O(=C) network in the stereocomplex.

1. Introduction

Poly(lactic acid) or polylactide (PLA) is a promising "green" plastic. The research interests in PLA arise not only from its environmentally benign synthesis and potential applications, but also from the great diversity of this polymer's chain architectures and crystalline structures. The precursor of PLA, lactic acid (2-hydroxypropanoic acid, $C_3H_6O_3$) is chiral, which leads to isotactic, syndiotactic and atactic/herterotactic PLA primary structures upon polymerization. The presence of repeating units with L- and D-opposite configurations in PLA polymer has been shown to provide a useful mean of adjusting physical and mechanical characteristics. PLA can be amorphous or crystalline, in general semicrystalline. Both poly(L-lactic acid) (PLLA) and poly(D-lactic acid) (PDLA) are isotactic, can crystallize in one of three polymorphs: α-, β- and γ-form [1–3]. More importantly, a 50–50 physical blend of PLLA and PDLA creates a new crystal structure – stereocomplex (sc)-form with a melting point T_m of 230 °C, about 50 °C higher than its individual components [4].

The structures of α [1,5–8], β [2,5,9], γ [3], and sc [3,4,10–12] forms have been solved by diffraction techniques combined with classical simulations. Empirical conformation analysis [1,13] and semiempirical molecular simulations (molecular mechanics (MM) [8,11,14], molecular dynamics (MD) [7,11] and rotational isomeric state (RIS) Metropolis Monte Carlo (RMMC) [15,16]) have been employed in investigating conformations and properties of PLA isolated molecular chains and their packing in a crystal. The studies showed that the lowest energy conformation of single PLLA chain is either left-handed helical 10_3 or 3_1. The chain packing and the intermolecular interactions in a crystal would disrupt the regular helical conformations. The destabilization of the α-helix type conformation was attributed to the repulsive electrostatic dipole–dipole interaction (electrostatic effect) between the dipoles associated to the ester groups [1]. In these classical studies, rigid structural parameters (i.e. fixed bond lengths and bond angles, values being taken from small molecules gas phase microwave structural analysis) were normally assumed. The ester bond was assumed planar trans and methyl group was simplified as a single

* Corresponding author. Tel.: +65 68748145; fax: +65 68727528.
E-mail address: cb-he@imre.a-star.edu.sg (C. He).

0032-3861/$ – see front matter © 2010 Elsevier Ltd. All rights reserved.
doi:10.1016/j.polymer.2010.03.062

sphere in some forcefields. Rotation angles around the backbone bonds O–C^{α} and C^{α}–C were the only degrees of freedoms. The advantages of these empirical methods are simple and fast, can be applied to large systems. However, the simulation results depend on the forcefields used: potential functions and parameters (partial charge assignment methods, L–J potential parameters, equilibrium bond lengths and angles etc, moreover, these parameters not being transferable). Hence it is very difficult to compare the results obtained using different forcefields. In contrast, no empirical input parameters and molecular geometry constraints are needed in quantum mechanics simulation, though it is computationally more intensive. Ab initio methods have been used to study lactides [17], amorphous PLA [18], oligomers (with repeat unit $n \leq 3$) [19,20] and their interactions with water [21]. However, to the best of our knowledge, there is no ab initio study done on crystalline PLA, except one done by the same authors of this work on elastic constants of single PLA crystals [22].

In this study, we present our systematic investigations on the energetic, structural, and electronic properties of PLA polymorphs by employing a quantum mechanical method in the framework of density functional theory (DFT) self-consistent field (SCF) calculations within the generalized-gradient approximation (GGA). Our objective is to provide a theoretical understanding on the mechanism of superior thermal stability through the forming of stereocomplex and the intermolecular interactions in PLA crystals. This work is organized as follows: In next section, we first discuss the computational methods in details. In Section 3, we present the results of our DFT calculations and findings. Finally, our conclusions are in Section 4.

2. Computational details

The initial structures of PLLA α-, β- and γ-form and PLLA: PDLA = 50:50 stereocomplex sc-form were built according to crystallographic data published in literature [3,5–9]. Hydrogen atoms were added to non-fully valent carbon atoms whenever necessary. Historically, three different unit cells have been proposed for PLLA α-form [6–8]. In order to clarify which one is energetically more favorable, we carried out DFT calculations for all of them. Details of the six starting PLA crystal structures built for DFT geometry optimization are summarized in Table 1. We shall refer to the denoted crystal structure codes in the subsequent sections.

Geometry optimization :relaxation of internal atomistic coordinates was carried out by using quasi-Newton method Broyden–Fletcher–Goldfarb–Shannon (BFGS) algorithm [23] within the constraints of lattice parameters and space group symmetry. We did not intend to optimize the cell sizes because the densities of the starting structures (in grams per cm^3): 1.260 (sc-form), 1.262 or 1.285 (α-form), 1.277 (β-form) and 1.312 (γ-form) as indicated in Table 1, are already in the range of experimental measurements: 1.290 g/cm^3 for crystalline, 1.248 g/cm^3 for completely amorphous [24].

Calculations were performed using DFT electronic structure programs DMol^3 [25,26] and CASTEP [27], both being available in the Materials Studio software suite (Accelrys Inc.). The nonlocal exchange-correlation:generalized-gradient approximation – Perdew–Wang functional (GGA-PW91) was used unless specified. Two different types (local and nonlocal) of basis sets were used. In DMol^3, numerical orbitals are used for basis functions, each function corresponding to an atomic orbital (AO). The double numerical plus polarization (dnp) with a global orbital cutoff of 3.7 Å was implemented because the dnp basis set is the most accurate and important for hydrogen bonding. For crystals, according to the Bloch's theorem, the periodic conditions make it simple to use a plane-wave basis set to expand the electron wave function. Implementation of plane-wave basis set in study crystal systems has two merits. The kinetic energy is diagonal and potentials are described in term of the Fourier transforms. Stresses and forces are computationally cheap in this approach. In CASTEP, a plane-wave basis set with an energy cutoff of 340 eV was employed for the geometry optimization; Core electrons are represented in pseudopotentials. Whereas norm-conserving psedopotentials – the density functional semicore pseudopotentials (dspp) generated by fitting all-electron relativistic DFT results – was chosen in DMol^3, the ultrasoft pseudopotentials (usp) was used in CASTEP because it is more efficient, with the lowest possible cutoff energy for the plane-wave basis set. The geometry optimization convergence tolerances of energy, maximum force, and maximum displacement are $1.0e^{-5}$ eV/atom, 0.03 eV/Å and $1.0e^{-3}$ Å, respectively.

3. Results and discussion

Unit cell total energy (E_{cell}) of PLA single crystal (α-, β-, γ- and sc-form) was calculated at DFT relaxed geometries. The structural and electronic properties were also determined at the optimized structures.

3.1. Unit cell total energy and comparisons

The calculated E_{cell} of various PLA crystals are given in Table 2. As the total energy is negative, when the absolute value is larger, the cell energy is lower and the corresponding crystal structure is more stable. For the three different proposed unit cells of α-form, the relative stability order is: α-form-2003 > α-form-2001 > α-form-1995.

Table 1
The six PLA crystal unit cells built based on the crystallographic data published in literature.

Crystal code	Crystal system; symmetry	Lattice constants (Å); angles (°); cell formula; density (g/cm^3)	Number of chains; conformation; packing	Monomers per chain; total monomers in the unit cell	Ref.
α-form-1995	Triclinic; P_1	a = 10.6[a], b = 6.1, c = 28.8; α = β = γ = 90; $C_{60}H_{80}O_{40}$; 1.285	2; left-handed 10_3 helices; parallel	10; 20	[6]
α-form-2001	Orthorhombic; $P2_12_12_1$	a = 10.6, b = 6.1, c = 28.8; α = β = γ = 90; $C_{60}H_{80}O_{40}$; 1.285	2; 10_3 helices; antiparallel	10; 20	[7]
α-form-2003	Orthorhombic; $P2_12_12_1$	a = 10.66, b = 6.16, c = 28.88; α = β = γ = 90; $C_{60}H_{80}O_{40}$; 1.262	2; Distorted helices; antiparallel	10; 20	[8]
β-form	Trigonal; P32	a = b = 10.52, c = 8.8; α = β = 90, γ = 120; $C_{27}H_{36}O_{18}$; 1.277	3; Frustrated left-handed 3_1 helices; parallel	3; 9	[9]
γ-form	Monoclinic; $P2_1$	a = 9.95, b = 6.25, c = 8.8; α = β = γ = 90; $C_{18}H_{24}O_{12}$; 1.312	2; 3_1 helices; antiparallel	3; 6	[3]
sc-form	Trigonal; R3c	a = b = 14.98, c = 8.8; α = β = 90, γ = 120; $C_{54}H_{72}O_{36}$; 1.260	6 (3 PLLA and 3 PDLA chains); 3_1 helices; parallel	3; 18	[3]

[a] In Ref. [6], a = 10.5 Å, here the lattice constant "a" is set to the same value (10.6 Å) as that of Refs. [5,7], for the convenience of comparison of energies between parallel and antiparallel packing.

Table 2
Energetic properties: unit cell total energy (E_{cell}), monomer energy $E_{monomer} = E_{cell}/N_{monomer}$ and relative energy ΔE (compared to sc-form) of PLA polymorphs at the levels of GGA-PW91-dspp/dnp (DMol^3) and GGA-PW91-usp/plane-wave basis set (CASTEP).

Form code	ΔE (kcal/mol) at the level of theory GGA-PW91-dspp/dnp (cutoff 3.7 Å)	ΔE (kcal/mol) at the level of theory GGA-PW91-usp/pw (cutoff 340 eV)
α-form-1995	1.7	2.3
α-form-2001	0.9	1.3
α-form-2003	0.4	0.6
β-form	1.1	1.3
γ-form	1.3	1.3
sc-form	0	0
The reference values	E_{cell}(sc-form) = −4809.9331985 hartree; $E_{monomer}$(sc-form) = −267.2185110 hartree	E_{cell}(sc-form) = −25372.0504 eV; $E_{monomer}$(sc-form) = −1409.5584 eV

Therefore, the distorted 10_3 helices and antiparallel packing α-form-2003 is the most stable among the three α-form unit cells.

A comparison of energies amongst dissimilar forms: α-, β-, γ- and sc-form is not straightforward because their unit cells hold different numbers ($N_{monomer}$) of PLA monomers ($C_3H_4O_2$) (refer to Table 1). So we normalized the cell energies to per monomer, $E_{monomer} = E_{cell}/N_{monomer}$ (i.e. total energy of a unit cell was divided by the number of monomers it contains). Table 2 shows that values of $E_{monomer}$ in the various forms are rather close to each other and the stereocomplex has consistently the lowest energy and hence is the most stable crystal structure of PLA no matter at which level of approximation. For the convenience of comparison, monomer energy difference between a homo-crystal and the stereocomplex is defined as $\Delta E = E_{monomer}$(α-, β-, or γ-form) − $E_{monomer}$(sc-form). According to this definition, $\Delta E > 0$ indicates a less stable structure than the sc-form. As shown in Table 2, the β-form and γ-form are energetically indistinguishable at the level of GGA-PW91-usp/plane-wave basis set with a energy cutoff of 340 eV. Increasing the plane-wave basis set energy cutoff from 340 eV to 380 eV when calculating single-point energies of the unit cells optimized at the cutoff 340 eV, and then we can get the difference. In addition, the energy (monomer) convergences of PLA polymorphs relating to the basis set energy cutoff are illustrated in Fig. 1(a) and (b) (where the alternative GGA-Perdew-Burke-Ernzerhof (PBE) functional and on the fly (otf) pseudopotentials were chosen to check the consistencies). The numerical values are available in Table S1 of the supporting information. For GGA-PW91-usp/pw, a cutoff of 380 eV is enough to differentiate the four PLA polymorphs correctly while for GGA-PBE-otf/pw the cutoff increases to 500 eV (minimum) to 610 eV. Hence using the ultrasoft pseudopotentials can reduce computation cost in the case of a plane-wave basis set.

In summary, the order of stability is as follows: sc-form (0) > α-form (0.3) > β-form (1.1) > γ-form (1.3) (DFT calculation at the level of GGA-PW91-usp/pw(cutoff 380 eV)//GGA-PW91-usp/pw (cutoff 340 eV)) or sc-form (0) > α-form (0.4) > β-form (1.1) > γ-form (1.3) (DFT calculation at the level of GGA-PW91-dspp/dnp (orbital cutoff 3.7 Å)). Hence, using either a localized numerical (dnp) or a delocalized plane-wave basis set, similar trend of relative stability for these PLA polymorphs can be predicted. When employ a plane-wave basis set, the energy cutoff must be large enough to ensure the energy convergence.

Earlier experimental studies show that the most common and stable phase of PLLA is α-form. The heat of fusion (H_f) of PLLA with 100% crystallinity was 93 J/g estimated by Fischer et al. [24]. (Higher values up to 148 J/g had been reported as well [28,29].) The melting temperature of PLLA is 185 °C [5] and equilibrium melting temperature (T_m^0) is 215 °C [30]. When drawing fibers of PLLA at a high draw ratio and temperature, α-form transformed to a less stable β-form [2], which has a melting point of 175 °C [5]. Different forms can coexist and one form can change into another under thermal or tension influence [2,5,31,32]. The sc-form has a much higher melting temperature, 230 °C [4]. H_f of stereocomplex had been established by Loomis et al., 142 J/g [28]. Kang et al. [33] had examined PLA stereocomplex by Raman spectra and concluded that C=O stretching bands were related to the packing formation of the polymer chain. By combining Raman spectroscopy and DSC techniques, they deduced H_f of stereocomplex to be 126 J/g. More recently Sawai at al reported the highest value of H_f (sc-form) 155 J/g [34]. The equilibrium melting temperature of sc-form is 279 °C [35,36]. Varied

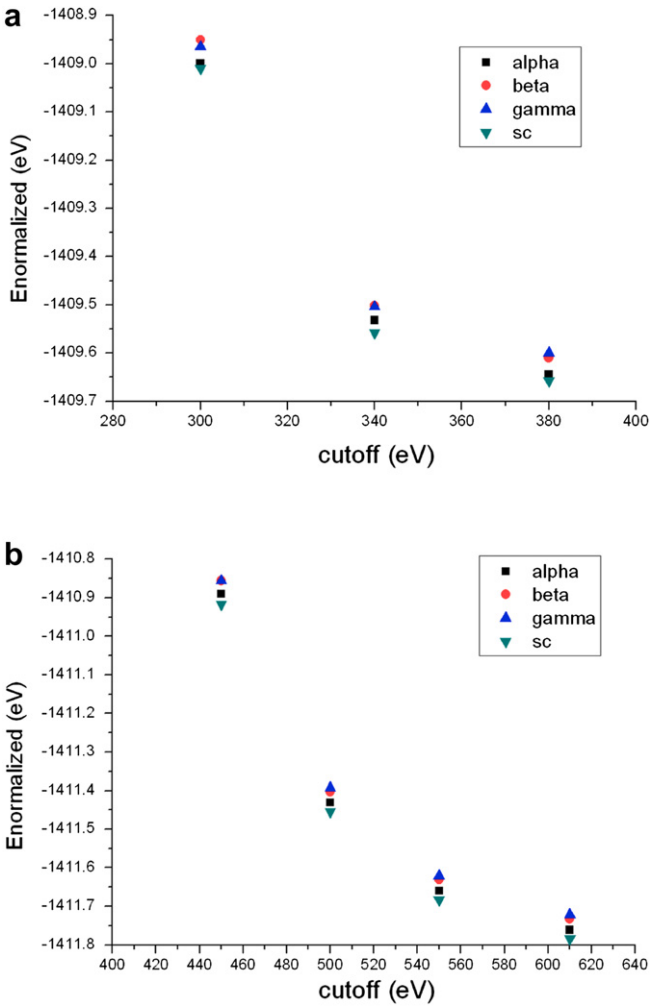

Fig. 1. Convergence of (monomer) energy of PLA with respect to basis set energy cutoff (a) GGA-PW91-usp/plane-wave basis set (cutoffs: 300, 340 and 380 eV) (b) GGA-PBE-otf/plane-wave basis set (cutoffs: 450, 500, 550 and 610 eV), calculated at unit cell geometries optimized at the level of GGA-PW91-usp/plane-wave basis set (cutoff 340 eV). In the legends, "alpha" means α-form-2003.

measured values of H_f and T_m^0 for same type of crystalline PLA may be caused by different molecular weights and sample preparation conditions and limited by the difficulty in obtaining pure infinite single crystals. Nevertheless, our theoretical calculated rank of relative stability of the PLA polymorphs is in agreement with some of the experimental studies: the melting temperature (differential scanning calorimetry (DSC) measurement) sequence: sc-form (230 °C, Ikata & Tsuji, 1987 [4]) > α-form (185 °C, Hoogsteen et al., 1990 [5]) > β-form (175 °C, Hoogsteen et al., 1990 [5]), the equilibrium melting temperature sc-form (279 °C, Tsuji & Ikada, 1996 [36], Tsuji, 2005 [35]) > α-form (215 °C, Kalb & Pennings, 1980 [30]); heat of fusion sc-form (155 J/g, Sawai, 2007 [34]) > α-form (93 J/g, Fischer, 1973 [24]); Activation energy for thermal degradation: PLLA/PDLA film (205–297 kcal/mol) > PLLA film (77–123 kcal/mol) (Tsuji & Fukui, 2003 [37]); scPLA-H (125–180 kcal/mol) > PLLA (80–120 kcal/mol) (Fan et al., 2004 [38]).

The intermolecular forces determining the packing of the polymer in crystal lattice apparently perturb the conformation of an isolated chain. Molecular symmetry and the non-bonded intra- or intermolecular interactions can affect the melting point, degree of crystallinity and glass transition temperature (T_g) [39]. Melting is a first-order thermodynamic transition, and the melting temperature, T_m, depends on the ratio of enthalpy and entropy of fusion $T_m = \Delta H_m/\Delta S_m$. Rigid molecules or molecules with strong intermolecular forces (e.g. hydrogen bonds) have high melting points due to low entropy of fusion. Poly(glycolic acid) or poly(glycolide) (PGA) is semicrystalline with high crystallinity (50%) and T_m (230 °C) and a T_g of about 40 °C. Early X-ray diffraction work revealed that the unit cell contains two antiparallel polymer chains and these chains have a sheet like molecular arrangement of planar zig–zag conformations. Also the C=O groups of the adjacent polymers in the unit cell overlap. The density of the crystal was determined to be rather high at 1.69 g/cm^3. It was suggested that the small $-CH_2$-group allows close packing and strong dipole interactions among esters, produces the abnormally high melting temperature and insolubility of the polymer [40]. In contrast to PGA, the pendant methyl groups force the PLLA chains to be helical (either 10_3 or 3_1). PLLA is also semicrystalline but with lower crystallinity (35–40%) and a lower T_m (180 °C), presumably due to methyl groups acting to partially shield dipole–dipole interactions. The T_g of PLLA is around 60 °C opposed to PGA 40 °C, as the bulky methyl group increases rotational barriers along backbone bonds (compared to PGA). PLLA is not flexible at lower temperature. For PLA sc-form, the higher melting temperature could arise from some additional special intermolecular interactions.

3.2. Molecular structural parameters

Tables 3 and 4 show (the averaged bond lengths, bond angles are available in Tables S2 and S3 of the supporting information) torsion angles of the PLA chain in various conformations: isolated helical 10_3 and 3_1 chains and their minor distortions in the crystals. While most of the DFT calculated bond lengths agree well with those reported empirical structural parameters, the calculated C^α–C^β (1.50–1.52 Å) is shorter than 1.54 Å. This is because in some forcefields or experimental characterizations, the methyl groups were generally treated as a united atom and hydrogen atoms of the methyl groups were expressed implicitly. In contrast, the calculated C^α–H^α length (1.09 Å) is longer than 1.07 Å (single chain). It is possible due to the hydrogen of C^α–H^α takes part in the non-conventional hydrogen bonding C–H···O=C in the crystals. The attractive interaction between the C–H and C=O may lead to the elongation of the C–H bonds. The assumption that the ester bond is planar trans is not definitely true in the crystals, the calculated torsion angle C^α–C–O–C^α is in the range of 167.5 to 175.1°, about 10° deviation from 180° (planar trans) except for γ-form. Our DFT calculated bond lengths are agree well with those reported by Blomqvist et al. [19,20]: C^α–C 1.523 Å, C–O 1.355 Å, C=O 1.212 Å, C^α–C^β 1.531 Å, which were calculated at the level of B3LYP/6–31 + (d) using a localized analytical Gaussian basis set for PLA oligomers (with one or two carbonyl groups); and those reported by Wu et al: C^α–O 1.449 Å, C^α–C 1.5296 Å, C–O 1.354 Å, C=O 1.204 Å, C^α–C^β 1.527 Å, C^α–H^α 1.101 Å, C^β–H^β 1.093 Å calculated at the level of B3LYP/6–31(d) for L-lactide [17]. The size of the numerical basis set dnp adopted by us is comparable to the polarized Gaussian basis set 6–31G(d, p).

Table 3
Structural parameters of PLA – helical 10_3 conformation of single chain or in a crystal unit cell.

10_3 helix	Single chain	α-form-1995		α-form-2001		α-form-2003	
	Refs. [13,41]	DMol^3	CASTEP	DMol^3	CASTEP	DMol^3	CASTEP
Torsion angle (°)							
O–C^α–C–O	160	155.9	155.5	160.4	159.9	161.7	161.6
C–O–C^α–C	−73	−66.9	−66.3	−67.0	−66.5	−68.5	−69.0
C^α–C–O–C^α	180	174.1	173.9	172.0	170.6	172.4	172.6

3.3. Population analysis – Mulliken charges

In classical mechanics simulation, to calculate electrostatic interaction terms in the forcefields, atomic charges must be specified. For some simple and small systems, the atomic charges can be inferred from experimental data or calculated using *ab initio* methods. For large systems like polymers, there are two methods for calculating approximate atomic point charges: the Gasteiger [42] and the charge equilibration (QEq) [43].

The calculated atomic charges are listed in Table 5. By utilizing the localized dnp basis set in the DFT calculations, we find that charges on H^α atoms in the sc-form are larger than those in α-, β- or γ-form. In addition, the charges on three H^β atoms of the same methyl group are unequal, particularly in sc-form. These are indications of forming intra- and/or inter-chain non-conventional

Table 4
Structural parameters of PLA – 3_1 conformation as a single chain or in a crystal unit cell.

3_1 helix	Single chain	β-form		γ-form		sc-form	
	Ref. [10]	DMol^3	CASTEP	DMol^3	CASTEP	DMol^3	CASTEP
Torsion angle (°)							
O–C^α–C–O	151.4/148.3	149.2	148.9	153.8	153.8	149.4	148.8
C–O–C^α–C	−75.0/−73.7	−71.2	−72.0	−71.8	−72.1	−71.4	−72.5
C^α–C–O–C^α	180	171.9	172.8	167.6	167.5	172.5	174.1
O–C^α–C–O	−151.4/−148.3					−149.4	−148.8
C–O–C^α–C	75.0/73.7					71.4	72.5
C^α–C–O–C^α	180					−172.5	−174.1

Table 5
Calculated atomic charges (unit: e) of PLA molecule in various forms.

DFT calculation at the level of GGA-PW91-dspp/dnp (orbital cutoff 3.7 Å)							
	O_carbonyl	O_ether	C^{α}	C^{β}	C(=O)	H^{α}	H^{β}
sc-form	−0.429	−0.416	0.007	−0.259	0.542	0.180	0.111, 0.145, 0.118
β-form	−0.424	−0.429	0.014	−0.279	0.551	0.163	0.138, 0.138, 0.128
	−0.422	−0.411	0.027	−0.278	0.537	0.144	0.143, 0.126, 0.137
	−0.428	−0.411	0.026	−0.261	0.537	0.145	0.131, 0.143, 0.110
γ-form	−0.425	−0.425	0.033	−0.294	0.544	0.157	0.129, 0.141, 0.149
	−0.413	−0.427	0.019	−0.292	0.541	0.150	0.133, 0.148, 0.135
	−0.426	−0.402	0.024	−0.298	0.538	0.151	0.139, 0.121, 0.140
α-form-2003	−0.412	−0.420	0.019	−0.266	0.553	0.149	0.108, 0.128, 0.146
	−0.427	−0.437	0.016	−0.266	0.555	0.154	0.119, 0.141, 0.127
	−0.442	−0.427	0.025	−0.266	0.556	0.153	0.129, 0.136, 0.129
	−0.416	−0.409	0.017	−0.290	0.546	0.162	0.128, 0.154, 0.122
	−0.409	−0.435	0.024	−0.265	0.549	0.148	0.117, 0.140, 0.136

hydrogen bonding in the polymer crystals and will be discussed further in the next section.

3.4. Non-conventional hydrogen bonding network

Brizzolara et al. [11] employed classical molecular mechanics (MM) method – Dreilding forcefield to study the sc-form formation mechanism. They ascribed the higher melting point of sc-form to the specific energetic interaction-driven packing caused by the van der Waals forces between helices in the stereocomplex. Zhang et al. [44] used infrared spectroscopy to explore the $CH_3\cdots O{=}C$ interaction in the sc-form. Their investigation indicated that the C=O stretching band of sc-form shows a 5 cm^{-1} low frequency shift during the melt-crystallization while that of PLLA does not. Tsuji et al. used solution [45] and solid-state [46] NMR to study the stereocomplex formation. They found that there are three resonance lines of the carbonyl carbons at 173.3, 172.0 and 169.7 ppm for the PLLA/PDLA blend. They assigned the component with spin-lattice relaxation time (T_{1C}) 128 s of 173.3 ppm to sc-form and 172.0 ppm $T_{1C} = 40$ s to homopolymer crystals. It has been shown that the weak (or non-conventional) hydrogen bonds [47] are important in biological systems [48,49] as well as small organic molecule crystallization [50]. Yates et al. have developed a quantitative method in characterizing the intermolecular C–H···O weak hydrogen bond [51]. They carried out first-principle calculations of ^1H chemical shift for a full crystal and an isolated molecule respectively and found a good correlation between the large chemical shift change and hydrogen bond geometry of both short H···O distance and large ∠CHO.

We added carbon C as a hydrogen bonding donor to the conventional donor–acceptor list (N, O, S, halogens as both donor and acceptor) and built the hydrogen bonds in the ranges of: maximum hydrogen-acceptor distance $d_{H\cdots O} < 2.72$ Å (the van der Waals radius for H and O is 1.20 and 1.52 Å, respectively. when the distance $d_{H\cdots O}$ is less than the sum of the atomic vdW radii, a H-bond may be formed) and minimum donor–hydrogen-acceptor angle

Table 6
Non-conventional H-bonding geometry ($d_{H\cdots O} < 2.72$ Å and ∠CHO > 80°) in PLA polymorphs (at DFT optimized structures) and calculated charges.

Crystal code	No. of H-bonds per repeat unit	H-bond type	Donor–acceptor	$d_{H\cdots O}$ (Å)	∠CHO (°)	q_H (e)	q_O (e)
sc-form	3	Intramolecular	$C^{\alpha}{-}H^{\alpha}\cdots O_{carbonyl}$	2.479	87.886	0.180	−0.429
		Intermolecular	$C^{\alpha}{-}H^{\alpha}\cdots O_{carbonyl}$	2.478	135.157	0.180	−0.429
		Intermolecular	$C^{\beta}{-}H^{\beta}\cdots O_{carbonyl}$	2.649	147.617	0.145	−0.429
α-form-2003	1.8	Intramolecular	$C^{\alpha}{-}H^{\alpha}\cdots O_{carbonyl}$	2.501	88.407	0.149	−0.409
				2.524	85.862	0.154	−0.412
				2.547	84.866	0.153	−0.427
				2.410	91.490	0.162	−0.442
				2.551	85.101	0.148	−0.416
			$C^{\beta}{-}H^{\beta}\cdots O_{ether}$	2.685	96.394	0.122	−0.435
		Intermolecular	$C^{\beta}{-}H^{\beta}\cdots O_{carbonyl}$	2.280	159.148	0.154	−0.442
				2.659	158.600	0.136	−0.427
			$C^{\beta}{-}H^{\beta}\cdots O_{ether}$	2.674	162.159	0.128	−0.435
β-form	2.167	Intramolecular	$C^{\alpha}{-}H^{\alpha}\cdots O_{carbonyl}$	2.442	90.059	0.163	−0.424
				2.484	88.103	0.144	−0.422
				2.503	86.961	0.145	−0.428
		Intermolecular	$C^{\beta}{-}H^{\beta}\cdots O_{carbonyl}$	2.485	134.973	0.143	−0.424
				2.715	137.437	0.138	−0.422
				2.397	125.548	0.126	−0.428
			$C^{\beta}{-}H^{\beta}\cdots O_{ether}$	2.436	148.565	0.143	−0.429
γ-form	2.333	Intramolecular	$C^{\alpha}{-}H^{\alpha}\cdots O_{carbonyl}$	2.483	90.187	0.151	−0.426
				2.411	89.323	0.150	−0.413
				2.428	90.417	0.157	−0.425
		Intermolecular	$C^{\beta}{-}H^{\beta}\cdots O_{carbonyl}$	2.506	134.812	0.141	−0.425
				2.661	127.019	0.129	−0.413
				2.696	145.097	0.133	−0.426
				2.683	113.794	0.135	−0.425

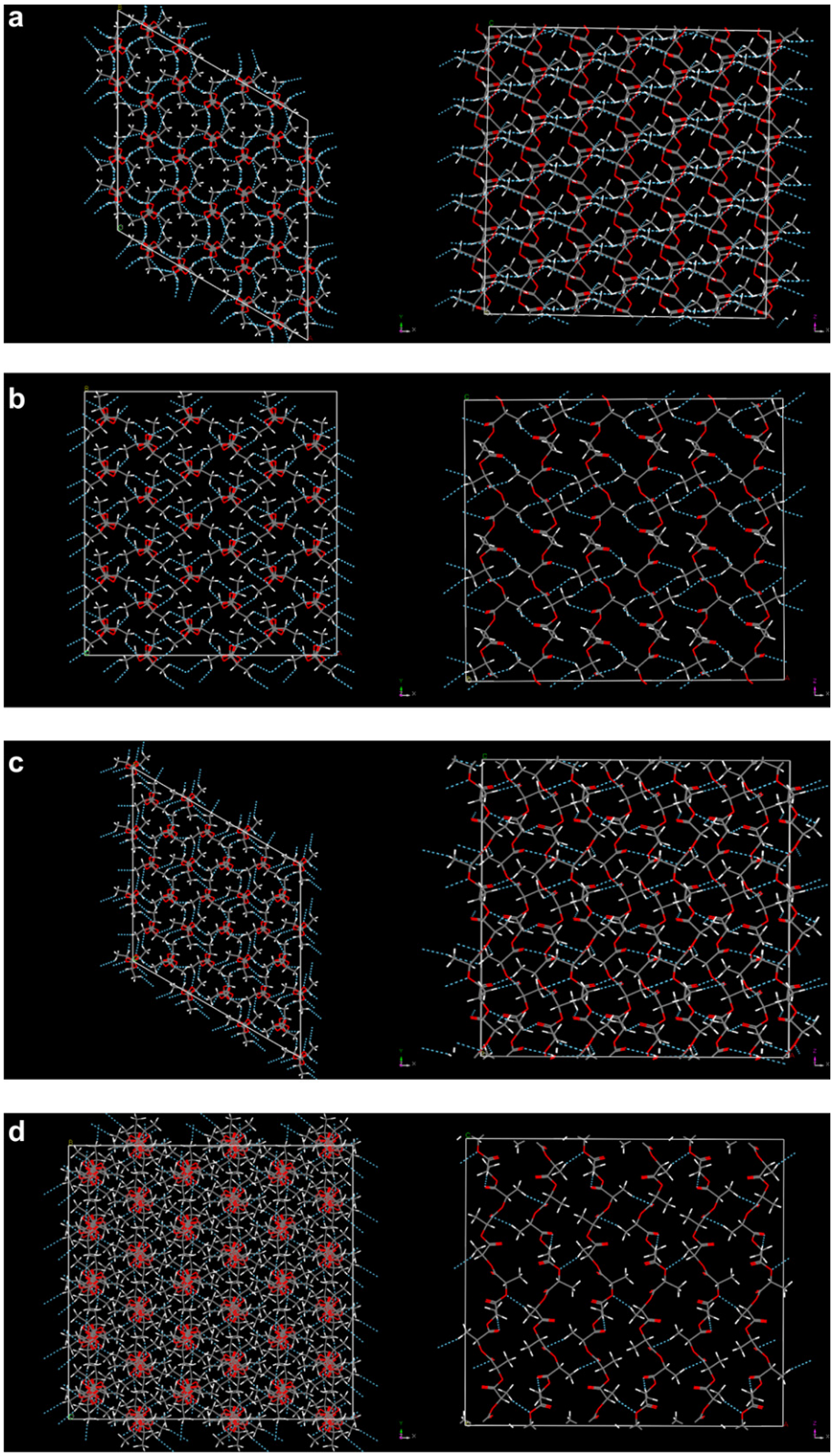

Fig. 2. Three-dimensional non-conventional hydrogen bonding C–H···O networks (light blue dotted lines, $d_{H\cdots O} < 2.72$ Å, $\angle CHO > 100^{\circ}$) in the PLA crystals: (a) the $2 \times 2 \times 3$ supercell of sc-form; (b) the $3 \times 5 \times 3$ supercell of γ-form; (c) the $3 \times 3 \times 3$ supercell of β-form. (d) the $3 \times 5 \times 1$ supercell of α-form. Element color codes: red – oxygen, white – hydrogen, and dark grey – carbon. Left panels are top view and right panels are side view of the supercells, helical chain axis along z axis (For interpretation of the references to color in this figure legend, the reader is referred to the web version of this article.).

$\angle$CHO > 80°. The non-conventional H-bonds geometry analysis for the PLA polymorphs is summarized in Table 6. The intramolecular H-bonds C^{α}–$H^{\alpha}\cdots O_{carbonyl}$ are in the short distance $d_{H\cdots O}$: 2.41 – 2.55 Å and almost acute angle $\angle$CHO: 84.9 – 91.5° ranges. Each PLA repeat unit has one such intramolecular H-bond regardless of crystalline form or chain conformation (either 10_3 or 3_1). However, the intermolecular H-bonds C^{α}–$H^{\alpha}\cdots O_{carbonyl}$ are only found in sc-form. Moreover the angle ($\angle$CHO) is obtuse (135.2°), which means more directional and the intensity would be higher. That also can explain why the atomic charges on the H^{α} atoms of sc-form are (about 0.03e) larger than those in the other three forms because each H^{α} takes part in two H-bonds C^{α}–$H^{\alpha}\cdots O_{carbonyl}$. The intermolecular C^{β}–$H^{\beta}\cdots O_{carbonyl}$ H-bond make the H^{β} more positively charged than the other two non H-bonded H^{β} atoms of the same methyl group. PLA in the sc-form has the highest number (three) of H-bonds per repeat unit. The three-dimensional H-bonding networks are illustrated in Fig. 2. For showing just the intermolecular H-bonds, we increased minimum angle $\angle$CHO > 100°. The 3D interconnecting and symmetric H-bonding network in sc-form is very notable. Such strong and unique H-bond network may contribute to the much higher melting point of sc-form. We shall carry out DFT calculations of solid-state NMR and IR to quantify and differentiate intensities of the intermolecular H-bonding interactions in these four PLA crystal structures.

4. Conclusions

We have carried out a systematic DFT investigation on the PLA polymorphs. The calculation results indicate that the sc-form is the most energy-favorable among the four PLA forms studied. The stability order is: $sc > \alpha > \beta > \gamma$, which is correlated to melting temperature: sc(230 °C) > α (185 °C) > β (175 °C). We provided a quantitative theoretical comparison. The huge increase in the melting point of the sc-form compared to other three homopolymer forms may attribute to the unique three-dimensional network of intermolecular non-conventional hydrogen bonding C^{α}–H···O(=C), $CH_3\cdots$O(=C) and $CH_3\cdots$O(ether) formed in the stereocomplex crystal. Further DFT calculations of solid-state NMR and IR are under investigations to quantify the intensity of the weak hydrogen bonding interaction in these four crystal forms of PLA. Structural and electronic properties of solid PLA have been calculated as well.

Appendix A. Supporting information

The energy (monomer) convergences of PLA polymorphs relating to plane-wave basis set energy cutoff. The DFT optimized bond lengths and angles of PLA. These data are available free of charge via the Internet.

Supplementary data associated with this article can be found, in the online version, at doi:10.1016/j.polymer.2010.03.062.

References

[1] De Santis P, Kovacs AJ. Biopolymers 1968;6:299.
[2] Eling B, Gogolewski S, Pennings AJ. Polymer 1982;23:1587.
[3] Cartier L, Okihara T, Ikada Y, Tsuji H, Puiggali J, Lotz B. Polymer 2000;41:8909.
[4] Ikada Y, Jamshidi K, Tsuji H, Hyon SH. Macromolecules 1987;20:904.
[5] Hoogsteen W, Postema AR, Pennings AJ, ten Brinke G, Zugenmaier P. Macromolecules 1990;23:634.
[6] Kobayashi J, Asahi T, Ichiki M, Oikawa A, Suzuki H, Watanabe T, et al. J Appl Phys 1995;77:2957.
[7] Aleman C, Lotz B, Puiggali J. Macromolecules 2001;34:4795.
[8] Sasaki S, Asakura T. Macromolecules 2003;36:8385.
[9] Puiggali J, Ikada Y, Tsuji H, Cartier L, Okihara T, Lotz B. Polymer 2000;41:8921.
[10] Okihara T, Tsuji M, Kawaguchi A, Katayama K, Tsuji H, Hyon SH, et al. J Macromol Sci Phys 1991;B30:119.
[11] Brizzolara D, Cantow HJ, Diederichs K, Keller E, Domb AJ. Macromolecules 1996;29:191.
[12] Cartier L, Okihara T, Lotz B. Macromolecules 1997;30:6313.
[13] Brant DA, Tonelli AE, Flory PJ. Macromolecules 1969;2:228.
[14] Brizzolara D, Cantow HJ, Mulhaupt R, Domb AJ. J Comput-Aided Mater Des 1996;3:341.
[15] Blomqvist J, Pietila LO, Mannfors B. Polymer 2001;42:109.
[16] Blomqvist J. Polymer 2001;42:3515.
[17] Wu W, Li W, Wang L, Zhang P, Zhang J. J Mol Struct: THEOCHEM 2007;816:13.
[18] McAliley JH, O'Brien CP, Bruce DA. J Phys Chem A 2008;112:7244.
[19] Blomqvist J, Ahjopalo L, Mannfors B, Pietila LO. J Mol Struct: THEOCHEM 1999;488:247.
[20] Blomqvist J, Mannfors B, Pietila LO. J Mol Struct: THEOCHEM 2000;531:359.
[21] Entrialgo-Castano M, Salvucci AE, Lendlein A, Hofmann D. Macromol Symp 2008;269:47.
[22] Lin TT, Liu XY, He CB. J Phys Chem B 2010;114:3133.
[23] Pfrommer BG, Cote M, Louie SG, Cohen ML. J Comput Phys 1997;131:233.
[24] Fischer EW, Sterzel HJ, Wegner G. Kolloid-Z u Z Polymere 1973;251:980.
[25] Delley B. J Chem Phys 1990;92:508.
[26] Delley B. J Chem Phys 2000;113:7756.
[27] Segall MD, Lindan PJD, Probert MJ, Pickard CJ, Hasnip PJ, Clark SJ, et al. J Phys: Condens Matter 2002;14:2717.
[28] Loomis GL, Murdoch JR, Gardner KH. Abstr Pap Am Chem Soc 1990;200. 2-POLY.
[29] Cohn D, Younes H, Marom G. Polymer 1987;28:2018.
[30] Kalb B, Pennings AJ. Polymer 1980;21:607.
[31] Sawai D, Takahashi K, Imamura T, Nakamura K, Kanamoto T, Hyon SH. J Polym Sci B Polym Phys 2002;40:95.
[32] Takahashi K, Sawai D, Yokoyama T, Kanamoto T, Hyon SH. Polymer 2004;45:4969.
[33] Kang SH, Aou K, Pekrul RL, Hsu SL. Abstr Pap Am Chem Soc 2002;224. 688-POLY.
[34] Sawai D, Tsugane Y, Tamada M, Kanamoto T, Sungil M, Hyon SH. J Polym Sci B Polym Phys 2007;45:2632.
[35] Tsuji H. Macromol Biosci 2005;5:569.
[36] Tsuji H, Ikada Y. Macromol Chem Phys 1996;197:3483.
[37] Tsuji H, Fukui I. Polymer 2003;44:2891.
[38] Fan YJ, Nishida H, Shirai Y, Tokiwa Y, Endo T. Polym Degrad Stabil 2004;86:197.
[39] Wnek GE. In: Wnek GE, Bowlin GL, editors. "Polymers" in encyclopedia of biomaterials and biomedical engineering. New York: Marcel Dekker Inc.; 2004.
[40] Chatani Y, Suehiyo K, Okita Y, Tadokoro H, Chujo K. Die Makrornolekulare Chernie 1968;113:215.
[41] Kang SH, Hsu SL, Stidham HD, Smith PB, Leugers MA, Yang XZ. Macromolecules 2001;34:4542.
[42] Gasteiger J, Marsili M. Tetrahedron 1980;36:3219.
[43] Rappe AK, Goddard WA. J Phys Chem 1991;95:3358.
[44] Zhang JM, Sato H, Tsuji H, Noda I, Ozaki Y. J Mol Struct 2005;735–736:249.
[45] Tsuji H, Horii F, Hyon SH, Ikada Y. Macromolecules 1991;24:2719.
[46] Tsuji H, Horii F, Nakagawa M, Ikada Y, Odani H, Kitamaru R. Macromolecules 1992;25:4114.
[47] Desiraju GR, Steiner T. The weak hydrogen bond in structural chemistry and biology. 1st ed. New York: Oxford University Press; 1999.
[48] Derewenda ZS, Lee L, Derewenda U. J Mol Biol 1995;252:248.
[49] Senes A, Ubarretxena-Belandia I, Engelman DM. Proc Natl Acad Sci U S A 2001;98:9056.
[50] Desiraju GR. Acc Chem Res 1991;24:290.
[51] Yates JR, Pham TN, Pickard CJ, Mauri F, Amado AM, Gil AM, et al. J Am Chem Soc 2005;127:10216.